CHAPTER 1

INTRODUCTION

This Chapter serves as an introduction to the thesis and the objectives of the current work. The first Section of the Chapter presents the current state and significance of knowledge on aerosol measuring related problems. The second Section presents a literature review of the already existing electrical aerosol instruments including the designs of unipolar chargers, the designs of mobility analyzers, and the development of electrical mobility analysis based instruments. The aims, benefits, and scope of the current study are also presented in the last Section of the Chapter.

1.1 Statement and Significance of the Problem

Particulate air pollution is one of the most important environmental topics. Automotive engines have long been recognized as a major source of particulate air pollution. Any solid or liquid material suspended in air with diameter in the range of 1 nm to 100 μm can be considered as a particle (Hinds 1999). These particles have significant effects on the human health, Earth's climate, air quality and processes in various industries such as food, pharmaceutical and medical, electronic and semiconductor industries. Important physical properties of airborne particles are size, number, surface area, density and shape. Knowledge of these properties of aerosols is of great practical importance in aerosol science, air pollution, process control industry and epidemiological studies among others. In air pollution studies, photochemical reactions in the atmosphere often begin with nanometer-sized particles. In nucleation and condensation processes which are the basic of many technological applications, nanometer particles serve as the incipient nuclei for many processes. In the electronic and semiconductor industry, the contamination control of nanometer-sized particles is needed to prevent the formation and deposition of these particles on semiconductor devices during fabrication because the size of the next generation 1-gigabit DRAM devices will have a minimum feature size smaller than 180 nm (Chen *et al.* 1998). Using the common 1/3 or 1/5 rule for microcontamination control, particles as small as 35 nm need to be measured and controlled. In industrial hygiene and epidemiological studies, the health consequences of these particulates depend on their ability to penetrate and deposit in the respiratory system. For particle size larger than 10 μm are screened out quite easy at the upper inhalation system. For particle in the size range between 1 to 10 μm can penetrate the alveoli and bypass the upper respiratory tract. Those particles are large enough that their terminal settling velocity allows deposition at places where they can do the most damage. Particles with a diameter of less than 1 μm can penetrate deep into the respiratory system to the human lungs and are difficult to remove by lung clearance mechanisms, and for this reason they are considered to be the most dangerous. There is therefore a need to develop efficient respirators for protecting workers exposed to environments containing nanometer sized particles. Measurement and characterization of these particles is therefore also needed in order to better understand and control them. A particle size instrument is one of valuable tool for these applications.

There are many instruments using various methods to measure particle size such as diffusion method, inertial impaction method, light scattering method, electron microscopy method and aerodynamic method. However, these techniques are only able to measure super-micrometer sized particles or painstakingly difficult and slow to obtain results for sub-micrometer or nanometer-sized particles. The most efficient and widely used technique

suitable for measuring these submicron particles is essentially an electrical mobility method. Electrical mobility method was initially developed to measure ions in gases (Zeleny 1898, 1900, 1929; Erikson 1921) and in the atmosphere (Erikson 1922, 1927; Chapman 1937). Rohmann (1923) later investigated and employed the method to measure atmospheric airborne particles. A good review of the historical development of the electrical aerosol measurements was given by Tammet (1970) and later by Flagan (1998). There have been numerous studies and developments on the electrical aerosol measurement in the past several decades. Among the first studies were by Whitby and Clake (1966), Tammet *et al.* (1973), Knutson and Whitby (1975) and Liu and Pui (1975). An electrical aerosol analyzer (EAA) and a differential mobility analyzer (DMA), capable of measuring 10 nm - 1 μm in diameter were developed and later improved and refined by a number of researchers such as Kousaka *et al.* (1983), Lehtimaki (1987), Stolzenburg (1988) and Winklmayr *et al.* (1991). Chen *et al.* (1997) used the numerical method to improve DMA design. The results were in good agreement with experimental data (Hummes *et al.* 1996). Seto *et al.* (1997) studied the performance of DMA under low pressure conditions to measure nanometer-sized particles in the size range between 4 - 10 nm. New developments were constantly tested and compared to assess their performance (e.g., Fissan *et al.* 1996; Brimili *et al.* 1997; Martinsson *et al.* 2001; Seol *et al.* 2002; Karlsson and Martinsson 2003) and to expand the measurement range. Kulon *et al.* (2001) described a bipolar charge aerosol classifier (BCAC). It uses electrostatic technique and is able to simultaneously measure particle charge as well as size. With respect to recent development on similar instrument, essentially an electrical mobility spectrometer (EMS), Tammet *et al.* (2002) designed and developed an electrical aerosol spectrometer (EAS) which is able to classify particles in a similar fashion to, but faster than a typical DMA due to its multi-channel measurement capability. Graskow (2001) developed a fast aerosol spectrometer (FAS) to measure nanometer-sized particles. His FAS prototype has better time response than the EAS. Reavell *et al.* (2003) and Biskos (2004) later reported a development of a differential mobility spectrometer (DMS), derived from Graskow's concept. Although these instruments are all designed to measure airborne particle size distribution using the same principles, they are also different in terms of specific applications, construction, cost, measurement range, as well as time response and resolution.

The objective of this thesis is to provide the design study and construct the prototype of an electrical aerosol size measurement system using an electrical mobility technique that measures aerosol particles in the size range 10 nm to 1000 nm. This thesis also investigates the aerosol transport under influence of an electric field inside the instrument and the factors which affect the aerosol measurement in sub-micrometer size range i.e. dimension of the instrument, fluid flow rate, electric field strength, particle charge distribution, and particle losses. The performances of the instrument are experimentally evaluated and comparison with the standard aerosol measuring instrument are discussed and presented.

1.2 Literature Reviews

1.2.1 Designs of Unipolar Chargers

(a) Corona-Wire Chargers

Hewitt (1957) was one of the first to develop and investigate experimentally a corona-wire diffusion charger to examine the charging process in the electrostatic precipitators. The charger consisted of a cylinder with a concentric corona wire placed along the axis, attached to the inner surface of the cylinder. A small path was formed to carry the aerosol flow. The main corona discharge volume and the aerosol flow region were separated by a metallic mesh, and an alternating voltage difference was applied between this mesh and the outer electrode of the charger to reduce particle losses. In his work, Hewitt conducted

experiments for particle in the size range between 60 to 700 nm and reported that the electric field strength resulted in high losses for particles with diameter as small as 70 nm.

Liu *et al.* (1967) experimentally studied the diffusion charging of aerosol particles by unipolar ions over the pressure range between 0.0311 and 0.960 atm using monodispersed aerosols of di-octyl phthalate (DOP). The experimental procedure consisted of exposing a monodispersed aerosol to unipolar ions produced by a high voltage corona discharge, and measuring the electrical mobility and charge of the aerosol in a straight-through, dynamic flow system. The schematic diagram of the diffusion charger used in the experiment is represented in Figure 1.1. It is similar to the charger, first described by Hewitt (1957). In Liu *et al.* charger, the aerosol was exposed to positive ions in the charging region which was bounded on one side by a solid electrode and on the other by a screen through which the positive ions produced by the corona discharge flow. An AC square-wave voltage was applied to the solid electrode to minimize the aerosol loss which occured in the charging process. The frequency of the AC square-wave voltage used ranged from 10 to 60 Hz and the amplitude of the square wave was kept low to permit the condition of pure diffusion charging to be approximated as closely as possible. In pure diffusion charging, the charge acquired by an aerosol of a given size at a given pressure was a function of two variables, N_0, the number concentration of small ions in the charging region, and t, the charging time, or the time during which the aerosol was exposed to ions. The number concentration of small ions in the charging region was measured by substituting a DC voltage for the AC square wave voltage and measuring the corresponding DC current which flowed through the screen into the charging region. The current was on the order of 10^{-9} to 10^{-6} A and was measured by means of a Keithley model 610A electrometer. It was found from the authors work that the experimental data was well represented by the equation

$$\frac{n_p}{d_p} = 9.0 \ln\left(1 + 1.02 \times 10^{-5} N_0 t d_p\right) \tag{1.1}$$

where n_p is the number of elementary units of charge on a particle (dimensionless), and d_p is the particle diameter in microns. The experimental data also shows Equation 1.1 agrees with White's equation.

Liu and Pui (1974) designed and experimentally studied the diffusion charger for monodisperse aerosols in the size range between 0.0075 μm and 5.04 μm. A schematic diagram of the diffusion charger is shown in Figure 1.2. The charger consisted of two concentric metal cylinders with a fine (25 μm diameter) tungsten wire placed along the axis of the cylinders. A positive high voltage was applied to the wire to generate a corona discharge field. The ions produced were either collected by the inner cylinder or flow through the screen opening on the inner cylinder to the annular gap space outside. In the annular gap space, the ions collided with the aerosol particles and caused the latters to become charged. In Liu and Pui charger, the total flow through the charger was fixed at 5 l/min (4 l/min aerosol + 1 l/min sheath air). The residence time of the charger was 0.217 sec. A sheath air flow was used adjacent to the inner cylinder in order to displace the aerosol stream away from the screen and to prevent aerosol particles from entering the high intensity corona discharge region within the inner cylinder. It was reported that the nominal $N_i t$ product was adjustable over a range from less than 1×10^6 to over 3×10^7 ions/cm^3 s.

Buscher *et al.* (1994) developed and investigated the unipolar diffusion charger for ultrafine particles. Figure 1.3 shows a schematic diagram of the new square wave charger. Its geometrical configuration was similar to the one used in the TSI EAA 3030.

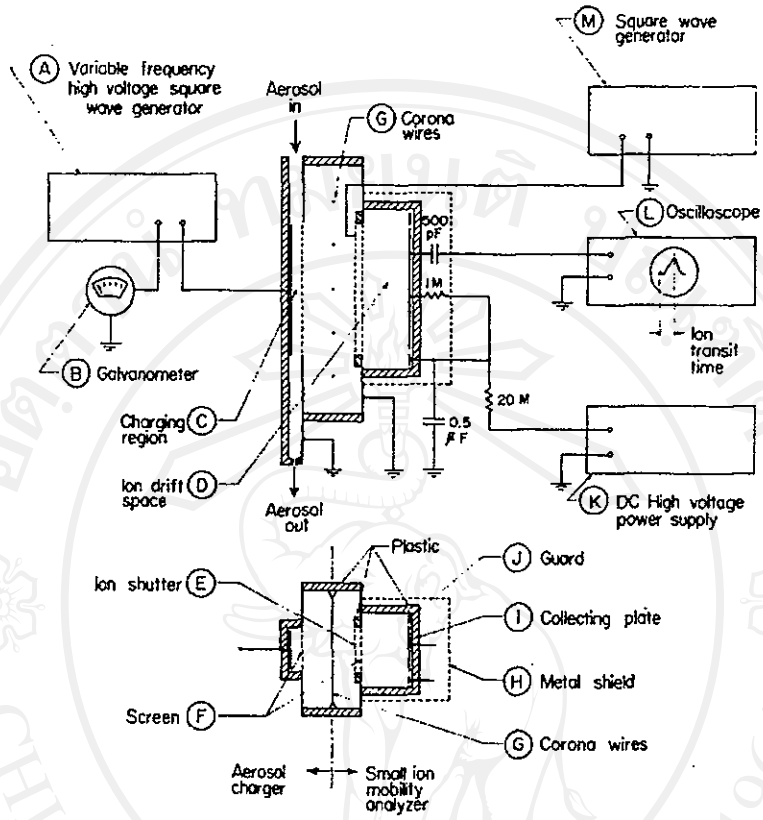

Figure 1.1 Schematic diagram of the diffusion charger developed by Liu *et al.* (Liu *et al.* 1967).

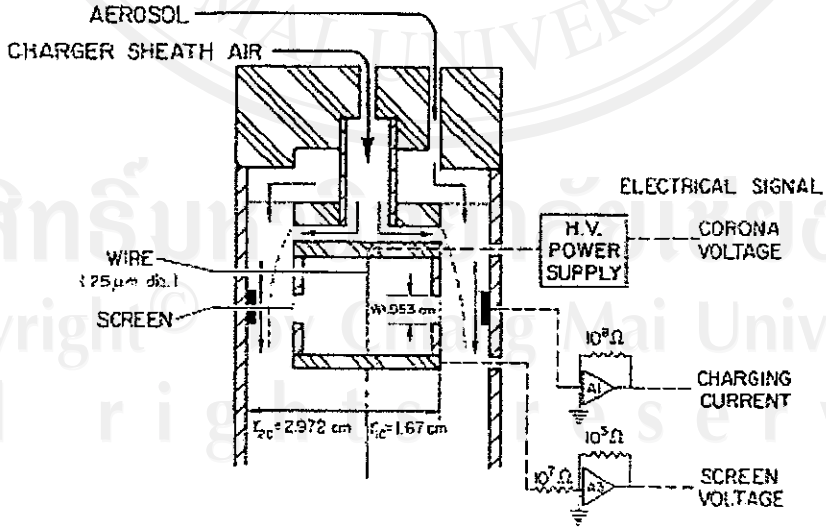

Figure 1.2 Schematic diagram of the diffusion charger developed by Liu and Pui (Liu and Pui 1974).

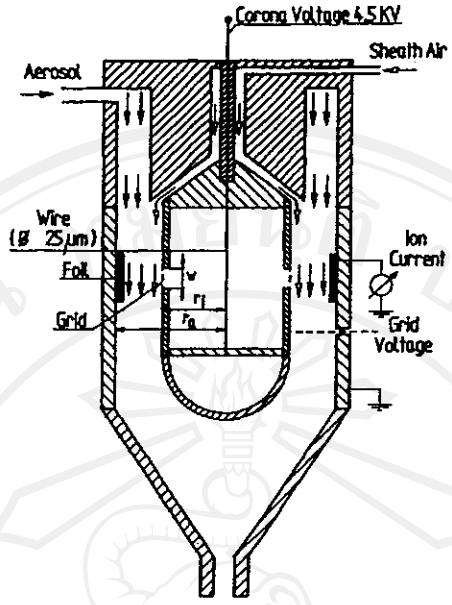

Figure 1.3 Schematic diagram of the square wave charger developed by Buscher *et al.* (Buscher *et al.* 1994).

However, the surfaces in contact with the aerosol were entirely conductive (stainless steel) and connected to ground, to avoid particle losses due to insulator charging. The inlet tubes for aerosol and sheath air was designed to achieve a high particle penetration and laminar flow inside the charger. A 4.5 kV corona discharge from a wire along the axis of the two concentric metal cylinders (radii r_i = 1.65 cm and r_a = 3.0 cm) produced ions. Applying a positive voltage to the inner cylinder, a grid (width w = 1.17 cm) permited ions from the discharge zone to enter the aerosol. The aerosol flowed into the annular gap space between the cylinders. The aerosol flow was 2 l/min and sheath air flow was 0.5 l/min. The sheath air surrounded the inner cylinder with the grid and prevented aerosol particles from entering the corona discharging zone. A square wave voltage was applied to the grid in the charging zone guaranteed minimized particle losses due to electrostatic force. An insulated foil on the inner side of the outer cylinder, opposite the grid, was connected to an electrometer amplifier for measure the charging current. In the experiment reported in Buscher *et al.* work, an evaporation nucleation generator was employed to generate polydisperse sodium chloride particles. A DMA type 3/150 was used downstream the generator to separate monodisperse samples from the polydisperse particles in the size range between 5 and 35 nm in diameter. Particle losses and charging efficiencies of the charger were determined by measure particle concentrations at the inlet and outlet of the charger. It was found from the authors work that the penetration decreased towards small particles where diffusion losses were highest, and the $N_i t$ product was approximately 1.1×10^7 ions/cm^3 s for the charger. The authors also reported that for the ion concentrations greater than 10^6 ions/cm^3, space charge had to be considered for the spatial dependence of the $N_i t$ product.

Unger *et al.* (2000) designed and tested the wire-cylinder corona charger for charged aerosol particles. The aim of this paper was to induce a stable negative corona discharge in flowing air with insulating surfaces near the active electrode. The second part dealed with the influence of the aerosol conditioning (concentration, flow rate) on the evolution of the discharge current (i.e. time life) related to the particles deposition on both the wire and the cylinder.

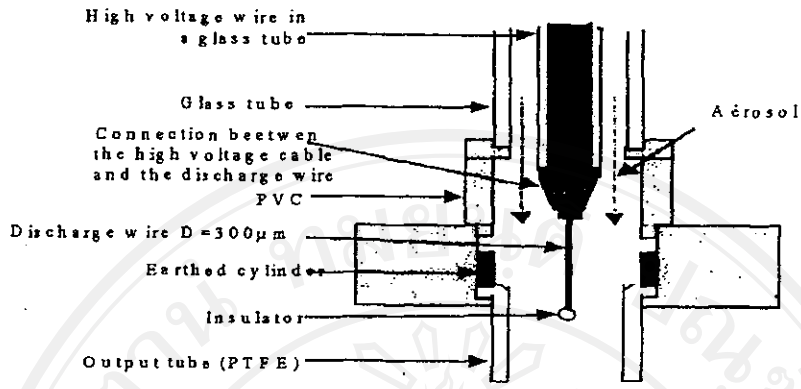

Figure 1.4 Schematic diagram of the wire-cylinder corona charger developed by Unger *et al.* (Unger *et al.* 2000).

Figure 1.4 shows a schematic diagram of the wire-cylinder corona charger. The wire diameter was 330 μm, and the grounded cylinder had an internal diameter of 14 mm for a length of 3 mm. With this electrode system, and with a voltage of -8.5 kV, the discharge current was about -30 μA, leading to ion densities in the range of 10^{10} ions/cm^3. The electrical measurements were obtained by oscilloscope connected to the cylinder for the discharge current and to a metallic foam for the charged particles output current. The tested aerosol was produced with a nebulizer and dried with a Silica-gel diffusion dryer. Granulometric characterization was achieved by DMA coupled with a CPC 3022. It was found from the authors work that an increase of the relative humidity implied a reduction of the discharge current by reduction of the ion mobilities leading to space charge accumulation in the discharge gap, lowering the electric field. The influence of the flow rate and the aerosol concentration affected the lifetime of the charger and the charged particles current at the output of the charger. High flow rate resulted in reduced particle losses in the charger and with nearly constant charging efficiency. Lower flow rate gave rise to a lower output current and a higher time of life.

Biskos *et al.* (2005) analytically and numerically investigated the electrostatic properties of aerosol corona-wire diffusion chargers, based on a Hewitt-type corona charger, at different operating conditions. Figure 1.5 shows a schematic layout of the unipolar corona-wire diffusion charger tested. It consisted of two concentric electrodes (50 and 74 mm in diameter) with a corona-wire placed along the axis. A 16 μm tungsten wire maintained at a positive high voltage was used to produce the corona discharge, while the generated ions migrated to the inner electrode due to the high electric field in the region. The inner electrode was made of a metallic mesh in order to allow ions to flow in the charging zone. An AC voltage applied on the outer electrode forced ions to enter the charging region without causing charged particles to precipitate on the charger walls, while the perforated inner electrode was connected to ground. The inner electrode maintained a laminar flow of the aerosol stream which was highly desirable for achieving a uniform residence time of the particles. Sheath air flowed in the ion generation area so that the axial pressure gradient of the two streams (aerosol and sheath flow) was the same. The aerosol flow passed through the annulus formed by the two cylinders, where the active charging region had a total length of 60 mm. The ammeter built into the high voltage power supply (Bertan series 230) was used to measure the current from the corona-wire electrode. For the charging zone, the 50 Hz AC filed voltage was coupled to the outer electrode via an isolating transformer. The other end of the secondary winding was connected to ground through a Keithley-617 electrometer in parallel with a 1 Hz high pass filter to allow measurement of the mean charging ion current.

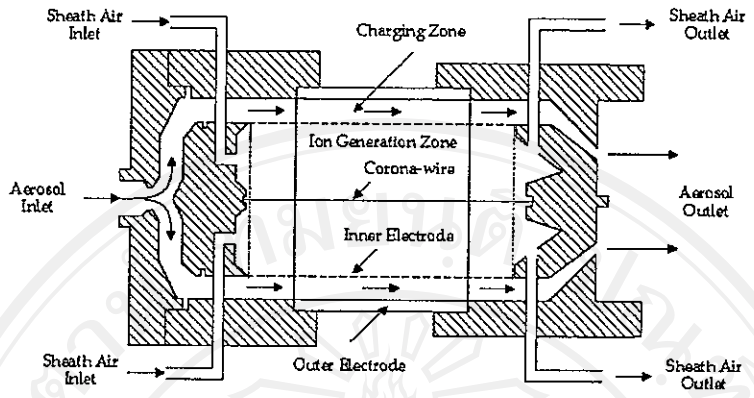

Figure 1.5 Schematic diagram of the unipolar corona-wire diffusion charger developed by Biskos *et al.* (Biskos *et al.* 2005).

Average and spatial distributions of ion concentrations for the two zones of the charger were calculated by a semi-empirical method based on ion current measurements, and presented the importance of considering the space charge effect in the analysis. The ion penetration through the perforated inner electrode of the charger was investigated by a numerical method. A finite element numerical solver (MATLAB PDE toolbox) was used for these types of calculations. The model consists of an axisymmetric finite element solution of Poisson's equation with Dirichlet boundary conditions applied on the side (corona-wire, inner and outer electrodes), and Neumann boundary conditions on top and bottom boundaries (sheath and aerosol flow inlets and outlets). The algorithm used a triangular grid with elements of varied size depending on the detail of the model at the different regions. It was reported that neglecting the space charge effect can lead to significant errors when the ion concentration in the charger is greater than 5×10^{13} ions/m^3. Estimation of ion penetration levels through the inner electrode based on the numerical model showed better agreement with the experimental results at sub-atmospheric pressures. Finally, calculations of the average $N_i t$ product appeared to increase with pressure, despite the fact that the ionic concentration was significantly lower.

(b) Corona-Needle Chargers

Whitby (1961) developed the first needle-type corona charger which was capable of converting the corona current into free small ions with 100% efficiency. A schematic of the sonic jet ion generator is shown in Figure 1.6. It consisted of an arrangement of a sharp needle held at high potential upstream of a small sonic orifice to generate the ions within a non-conductive housing. Clean air entered at inlet and then passes through the orifice plate. Positive, negative, or alternating current voltages on the needle electrode with respect to orifice plate used to produce positive, negative, or a mixture of positive and negative ions. It was reported that the ion generator produced unipolar or mixed positive and negative ion concentration of up to 10^{11} ions/cm^3 in the charging zone and total ion outputs of 10^{14}/sec had been achieved using 70 l/min of free air at 2 atm through a 1.59 mm. orifice diameter.

Medved *et al.* (2000) developed a new corona jet charger for aerosol particles. A schematic diagram of the corona jet charger is shown in Figure 1.7. It was currently employed by the Electrical Aerosol Detector (TSI 3070A). Ions were generated at a corona needle tip located in a small ion-generation chamber which was connected to a mixing chamber via an orifice.

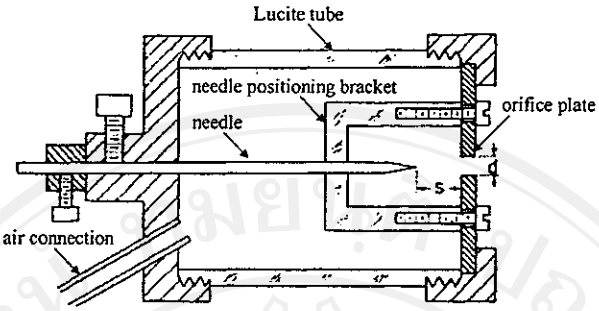

Figure 1.6 Schematic diagram of the sonic jet ion generator developed by Whitby (Whitby 1961).

The chamber where the corona discharge generates ions was isolated from a field-free mixing chamber where the aerosol was exposed to the ions. An air flow transfered the ions into the mixing chamber, and an opposing aerosol flow promoted mixing of the aerosol and the ions. The design created turbulent conditions in the mixing chamber. Since the aerosol-ion mixture was not subjected to an applied electric field, the only field being a negligible one was from the ion space charge itself. It was reported that particles were more efficiently charged, compared to corona-wire chargers due to better turbulent mixing.

Marquard *et al.* (2003) designed and investigated a twin corona-needle charger. A schematic diagram of this charger is shown in Figure 1.8. It was a twin corona module charger consisting of a cubic chamber made of polyethylene (w × h × l: 70 × 90 × 120 mm) with two charging modules placed on opposing side walls perpendicular to the main flow (11 or 20 l/min, respectively). Within these modules, ions were generated in a point-ring corona configuration (1 cm gap, ring diameter 15 mm) based on the ion gun concept of Whitby (1961) and transported by humidified air (50% RH; 1, 10 or 20 l/min, respectively) through the ring into the particle charging chamber. Inside the charger, additional metallic plates were placed around the corona module holes. Particle residence times were approximately 3 s < t < 10 s, dilution ratios resulting from the corona flows were 1.1 < f < 1.9. The device reported high charging efficiencies for sub-100 nm particles.

Hernandez-Sierra *et al.* (2003) designed, constructed and evaluated a very simple corona-needle charger, useful for high efficiency unipolar charging of nanometer-sized aerosol particles. Figure 1.9 shows the schematic diagram of the unipolar corona ionizer. It consisted of a cylindrical tube with tapered ends, and divided into three sections. The first and second ones were made of methacrylate, and the third of aluminum. A circular piece made of Teflon, placed between the two methacrylate sections, contained a series of orifices through which the aerosol flows. This central piece served to hold a stainless steel needle electrode, ending in a sharp tip, coaxial with the external cylinders. The electrode head was connected to a DC high voltage power supply, while the outlet metallic section was grounded. Charging experiments were carried out using the setup represented in Figure 1.10. Nanometer-sized NaCl particles were generated by a conventional evaporation-condensation technique. The number concentration of ions leaving the ionizer was represented in Figure 1.11, as a function of the corona voltage. Negative corona appeared at about 2.6 kV, while the positive corona was about 3.2 kV. It was reported that the charging efficiencies of positive and negative corona as high as about 30% for 10 nm particles. The charging efficiency also increased with particle size, corona voltage and mean aerosol residence time in the charger. At high corona voltage, the electrostatic deposition of charged particles within the charger was relatively high.

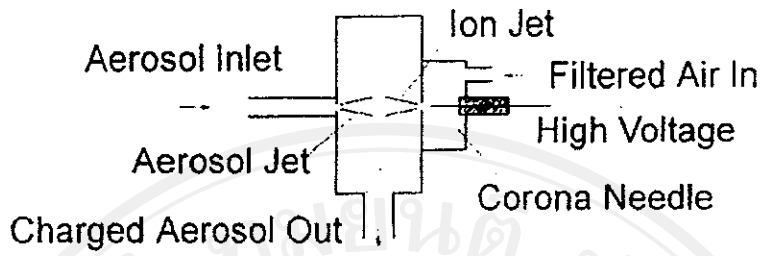

Figure 1.7 Schematic diagram of the corona jet charger developed by Medved *et al.* (Medved *et al.* 2000).

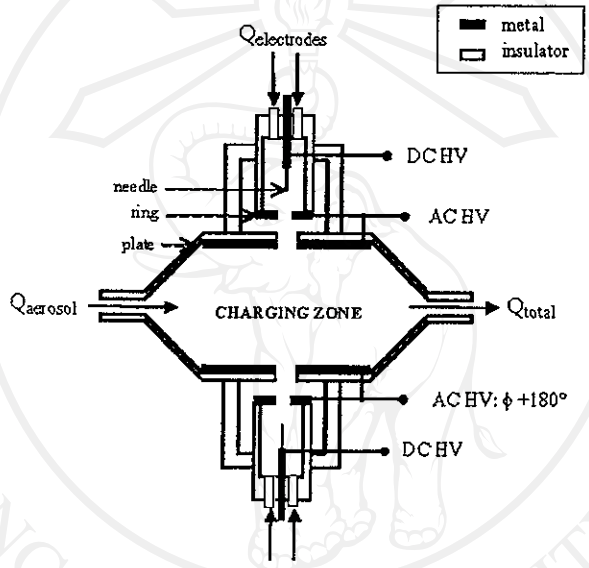

Figure 1.8 Schematic diagram of the twin corona module charger developed by Marquard *et al.* (Marquard *et al.* 2003).

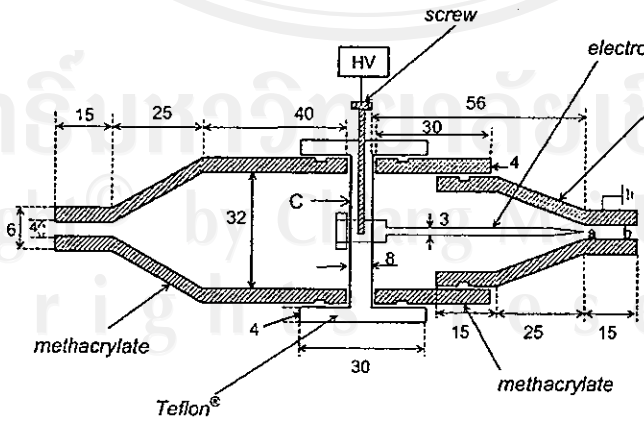

Figure 1.9 Schematic diagram of the unipolar corona ionizer developed by Hernandez-Sierra *et al.* (Hernandez-Sierra *et al.* 2003).

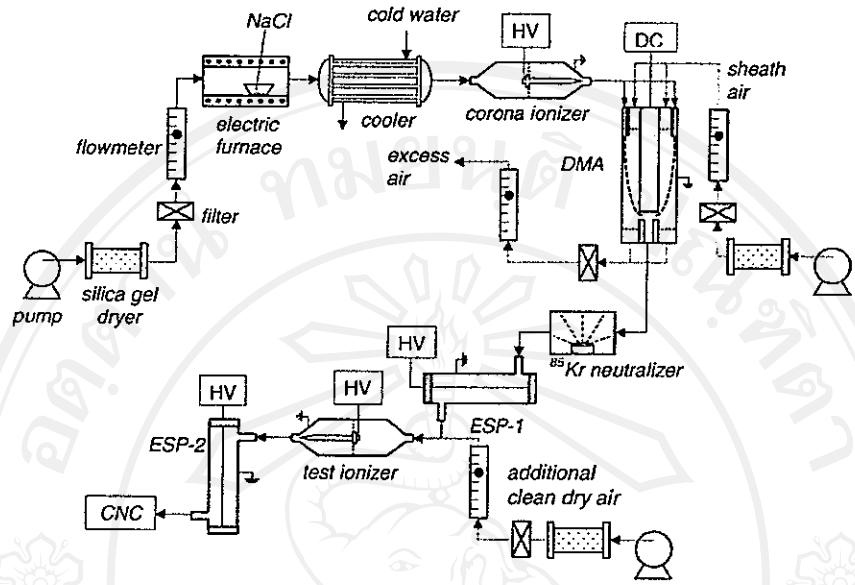

Figure 1.10 Experimental setup of the measurement of charging efficiency (Hernandez-Sierra *et al.* 2003).

The device reported the extrinsic charging efficiencies of this charger were almost one order of magnitude higher than the corresponding steady-state charging efficiencies attainable in bipolar radioactive chargers, and practically the same as those achievable with unipolar chargers of comparatively more complicated designs as shown in Figure 1.12 and 1.13.

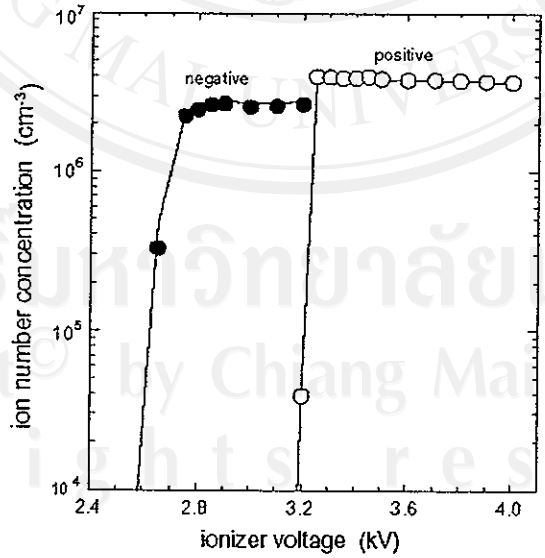

Figure 1.11 Total ion number concentrations at the charger outlet (Hernandez-Sierra *et al.* 2003).

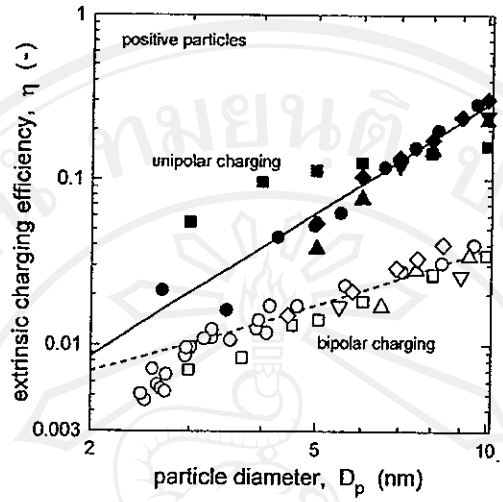

Figure 1.12 Charging efficiency of the corona-needle charger as a function of particle size for positive particles. Comparison between unipolar charging (solid symbols) and bipolar charging (open symbols): ● Hernandez-Sierra *et al.* (2003) work; ▲ Buscher *et al.* (1994); ▼ Wiedensohler *et al.* (1994); ■ Chen and Pui (1999); ♦ Kruis and Fassan (2001); ◊ Hussin *et al.* (1983); ∇ Adachi *et al.* (1985); Δ Wiedensohler and Fissan (1991); □ Reischl *et al.* (1996); ○ Alonso *et al.* (1997) (Hernandez-Sierra *et al.* 2003).

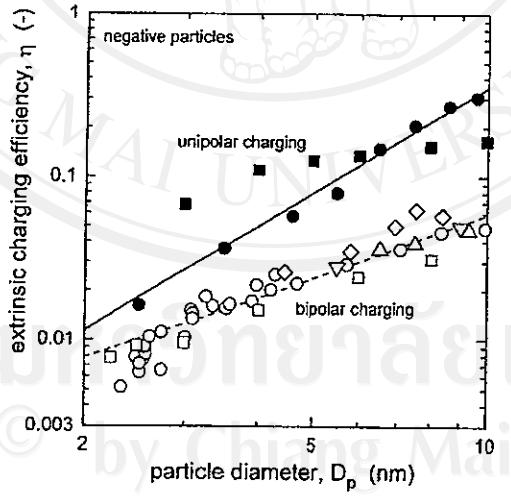

Figure 1.13 Charging efficiency of the corona-needle charger as a function of particle size for negative particles. Comparison between unipolar charging (solid symbols) and bipolar charging (open symbols): ● Hernandez-Sierra *et al.* (2003) work; ■ Chen and Pui (1999); ◊ Hussin *et al.* (1983); ∇ Adachi *et al.* (1985); Δ Wiedensohler and Fissan (1991); □ Reischl *et al.* (1996); ○ Alonso *et al.* (1997) (Hernandez-Sierra *et al.* 2003).

1.2.2 Designs of Mobility Analyzers

Knutson and Whitby (1975) improved the Hewitt (differential) electric mobility analyzer and presented the basic theory of aerosol classification by electrical mobility. The mobility analyzer used in the experimental part of Knutson and Whitby study is shown in Figure 1.14. It was a coaxial cylinder arrangement with two flow inlets and two outlets, similar to that used by Hewitt (1957). Clean air entered the mobility analyzer through the axial pipe at the top of the analyzer. This air flowed downward through the axial hole in the two plastic pieces, then outward through the eight 0.239 cm diameter. The flow continued axially downward through a 74 μm mesh nylon screen in order to evenly distribute and smooth the clean air flow before it entered the annular space between the mobility analyzer center rod and the mobility analyzer housing. The aerosol flow entered the mobility analyzer, and then flowed axially downward through a narrow annular space (gap = 0.159 cm), which distributed the aerosol evenly to all sectors of the mobility analyzer. At the bottom of this annular space was a circumferential gap, through which the aerosol entered the main analyzing region of the analyzer and met the clean air flow. The clean air flow forced the aerosol to flow downward in a thin layer on the outer wall of the analyzing region. It was essential that these two streams merged smoothly without mixing. A small portion was withdrawn through a circumferential groove (0.159 × 0.159 cm) near the bottom of the center rod. This sample flowed through the twelve 0.159 cm diameter. Particle with high electrical mobility deposited on the center rod upstream of the sampling slit. Those with low mobility were carried out with the main outlet flow. In between, three exits a narrow range of mobility for which the particles reached into the sampling slit and were carried out with the sampling flow. The early applications of the device were primarily as a source of relatively monodisperse aerosol for the calibration of instruments such as the condensation nucleus counter and the EAA. Calibration of the instrument using polystyrene latex particles revealed that the shape of the transfer function was closely reproduced for relatively large particles as shown in Figure 1.15.

Lehtimaki (1987) developed a new measuring technique for electrical aerosol analyzer. The special feature of this method was the current measuring technique which made it possible to continuously measure the electric current collected by the mobility analyzer. This measuring system consisted of a zeroth-order mobility analyzer and an electrometer current sensor. The principle of the zeroth-order mobility analyzer was similar to the one used in ion meters (Israel 1970). The schematic diagram of the measuring system is shown in Figure 1.16. The system consists of an aerosol charger, a mobility analyzer and filter charger collector. The aerosol charger is similar to that used in the electrical aerosol detector (EAD) (Lahtimaki 1986). In the charger, ions were generated by a corona discharge in a needle electrode installed inside a cylinder with a radius of 3.8 cm. The zeroth order mobility analyzer consisted of a coaxially cylindrical electrode (radii 2.5 cm and 3.0 cm). The sample air flow of 75 l/min was drawn through the space between these two electrodes. The mobility analyzer was installed inside the grounded metallic tube. PTFE insulator rings were used to isolate the analyzer from the ground potential. The DC high voltage power supply was installed inside the inner electrode which functions as the voltage electrode. The length of the voltage section of the inner electrode was 13.0 cm. The continuous power transfer to the floating high voltage supply was realized by means of the isolation transformer. The filter charge collector consisted of an electrical isolated filter element connected to the electrometer amplifier. The experimental studies were carried out in a small test room with the volume of 28 m^3. DOP (dioctyl phthalate) particles generated by a condensation type generator were used as test aerosol. The NaCl (sodium chloride) particles generated by a nebulizer as well as cigarette smoke particles were used in some measurements. The particle sizes of the test aerosols were determined by the EAA and the optical particle analyzer (PMS LAS X).

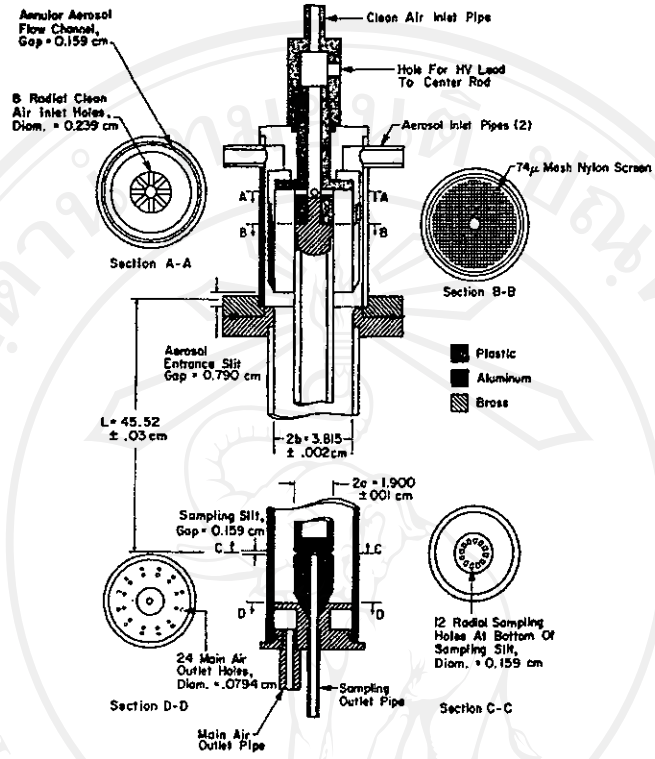

Figure 1.14 The mobility analyzer developed by Knutson and Whitby (Knutson and Whitby 1975).

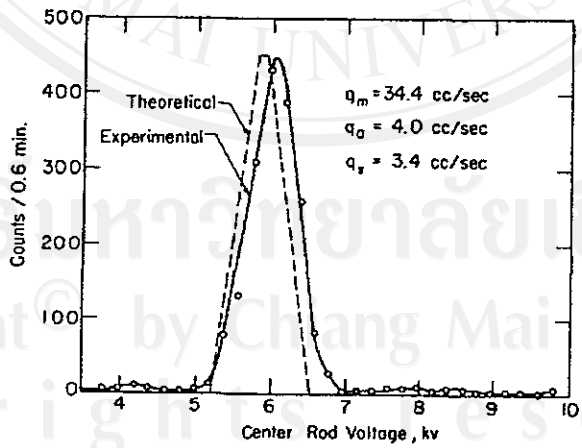

Figure 1.15 Comparison of the transfer function for the DMA predicted by Knutson and Whitby with their measurement using monodisperse polystyrene latex aerosol (Knutson and Whitby 1975).

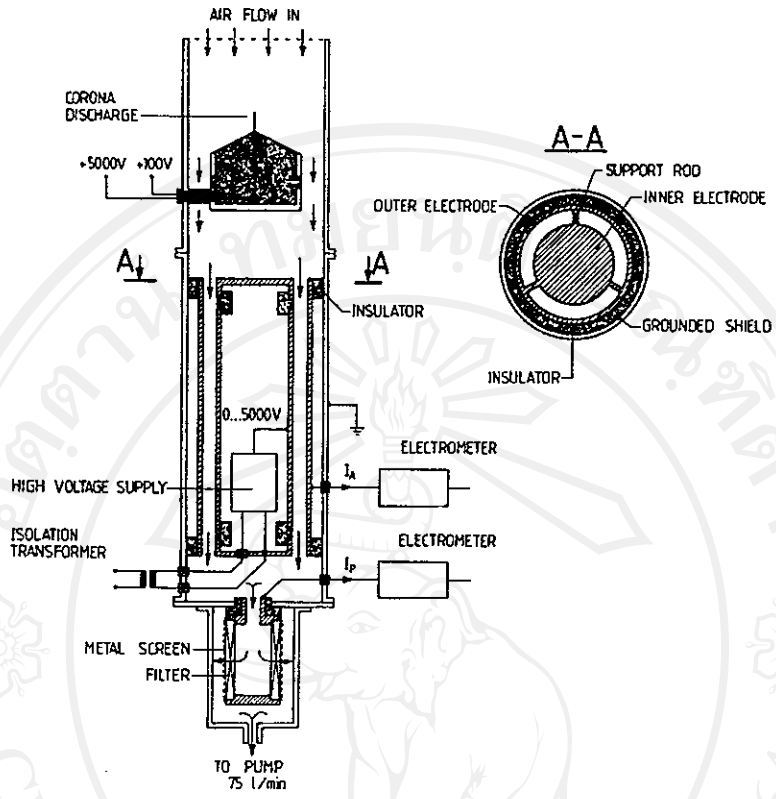

Figure 1.16 Schematic diagram of the analyzer developed by Lehtimaki (Lehtimaki 1987).

The size range of the particles extended from 0.02 μm to 1.2 μm. The geometric standard deviation of the particle size distributions varied from 1.3 (DOP) to 2.5 (NaCl). It was found from the author work that the collecting voltage of the analyzer can be varied in the range between 0 – 5000 V and simultaneously it was possible to measure the collected electric current down to 0.01 pA.

Winklmayr *et al.* (1990) developed the new types of the DMA (the University of Vienna DMA) for the size classification of fine and ultrafine aerosols. Figure 1.17 shows a schematic cross-section of the University of Vienna DMA. The aerosol was introduced tangentially into the annular region around the aerosol entrance slot to provide a uniform distribution of aerosol particles while keeping particle losses small. The sheath air was introduced through a nylon mesh screen above the central electrode and then entered into the classification region. In the original version, the outlet was connected directly to an extremely sensitive Faraday cup electrometer detector with sensitive of 10^{-16} A, again minimizing particle losses. A multi-stage cascade impactor works as a precut device. This system was designed for classification of particles in the size range of 3 to 150 nm in diameter, but had also been applied to measurements in the 1 to 40 nm size range.

Chen and Pui (1997) developed a numerical model to predict the performance of DMA for nanometer sized aerosol measurements. The model took into account the diffusion broadening and loss effects caused by particle Brownian motion. It was used to predict the transfer functions of TSI-short DMA under the flow condition of 1.0 l/min aerosol flow and 10.0 l/min sheath air flow rates for particle sizes between 5 and 50 nm. This model consisted of three parts: flow field, electric field, and aerosol transport formulations.

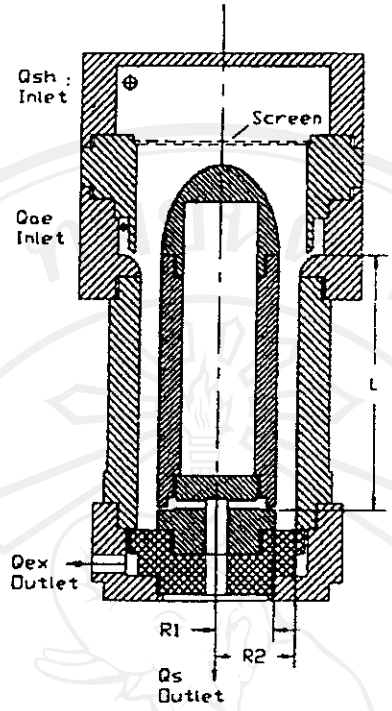

Figure 1.17 The University of Vienna DMA (Winklmayr *et al.* 1990).

For flow field modeling, Chen and Pui assumed that the flow inside the DMA was steady, incompressible and laminar. Based on these assumptions, the continuity and incompressible Navier-Stokes equations (N-S equation) were used in this model. For the boundary conditions used, no slip boundary was applied to all the solid walls included in the computation domain. Uniform velocity profile was assumed at the aerosol inlet. The velocity profile at the aerosol outlet was assumed to have the same profile as the nearest-neighboring cross section while keeping the total flow volume conserved. For electric field modeling, Chen and Pui assumed that the space charge effect on the electric field inside the DMA was neglected for low aerosol concentration, typically less than 10^6 particles cm^{-3}, and with low particle charge level. For the boundary conditions used, constant electric potentials were applied to the inner ($\Phi = U$) and outer ($\Phi = 0$) electrodes and the zero gradient condition was applied to the boundaries without walls. For aerosol transport and transfer function modeling, the convective aerosol transport equation with external electrical force was used. The aerosol transport inside the DMA was assumed to be steady if the aerosol inlet concentration was kept constant. In terms of the boundary conditions, zero concentration was applied to all the solid walls. Uniform concentration profile was used at the aerosol inlet, and zero concentration gradient in the flow direction was applied at the exit. Numerical approach had to be taken in order to obtain the solutions. A hybrid finite-element method was used. Mixed Galerkin and streamline upwind/Petrov-Galerkin (SUPG) finite-element formulations with a nine-node velocity, three-node pressure flow elements and bilinear element were used. The electric field equations were solved by the Galerkin finite-element method with the second-order isoparametric element. A modified adaptive characteristic Petrov-Galerkin finite-element method was proposed to overcome the difficulty involved in numerically solving the simplified equation. The numerical results clearly demonstrated the Brownian diffusion effect on the performance of the DMA. The effect significantly deteriorated the sizing resolution and the detection sensitivity of the DMA when measuring nanometer sized aerosols. They were then validated

by comparing the numerical and experimental results for simulated scans from two DMA operating in series. It was reported that the numerical transfer functions were compared with the available experimental data from two sources, namely, Hummes *et al.* (1996) and Kousaka *et al.* (1986). A good agreement between them was obtained in the comparison.

Seto *et al.* (1997) developed a low pressure differential mobility analyzer (LPDMA) with a Faraday cup electrometer (FCE) for measuring nanometer sized aerosol particles. Figure 1.18 shows a schematic diagram of the LPDMA developed by Seto *et al.* This LDMA was similar to that of the Vienna DMA. The aerosol particles were charged using bipolar ions which were generated by α-ray irradiation using ^{241}Am in an aerosol bipolar charger. The bipolar charging of nanometer sized particles at low pressure was analyzed by theoretical calculation using Fuchs theory. The equilibrium charge distribution obtained at low pressure was used to calculate the size distribution from the mobility distribution. The performance of the LPDMA was investigated experimentally using a tandem DMA technique as shown in Figure 1.19. The monodisperse silver particles were used as test particles. It was found from Seto *et al.* work that LPDMA can be used to measure nanometer-sized particles in the range between 4 – 10 nm under low pressure conditions in the range of 60 – 760 Torr. This technique can be applied to measurement of nanometer sized particles and ions in physical vapor deposition (PVD) and low pressure chemical vapor deposition (LPCVD) systems.

Chen *et al.* (1998) developed and optimized a nanometer aerosol differential mobility analyzer, Nano-DMA, for measuring the size distribution of nanometer aerosols in the particle size range of 3 to 50 nm. A schematic diagram of the Nano-DMA is shown in Figure 1.20. The design was based on a cylindrical configuration and was optimized by means of the numerical model of Chen and Pui (1997). Important design features included high particle penetration (low loss) through the Nano-DMA and high sizing resolution. For reducing particle loss the aerosol transport passage, the aerosol residence time in the Nano-DMA was reduced by shortening the inlet transport passage. An optional feature of high inlet flow was designed in order to further reduce the residence time between the aerosol inlet and the slit in the classifying region of the Nano-DMA. A new entrance slit was designed to have optimal aerosol and sheath air flow matching at a flow ration of 1 : 10, and had a wide dynamic flow-ration range (up to aerosol/sheath flow ratio of 1/70) compared with the TSI-standard DMA design. This slit improvement made the Nano-DMA suitable for high resolution particle sizing and classification. For reducing the effect of Brownian diffusion broadening on the transfer function of the Nano-DMA, the collector tube length was shortened to 5.0 cm compared to the TSI-standard DMA of 44.44 cm and TSI-short DMA of 11.11 cm. At the design flow condition of 1.5 l/min aerosol and 15.0 l/min sheath air flow rates, the measurement size range was from 3 – 50 nm. The lower detection limit of 3.0 nm coincided with the lower detection limit of the TSI UCPC. The base of the Nano-DMA was completely re-designed to avoid particle loss due to the undesirable electrostatic effect observed by Kousaka *et al.* (1986), and to obtain an uniform electric field in the entire classifying region. The overall performance of the Nano-DMA was then evaluated by the numerical model of Chen and Pui (1997) before its construction and experimental evaluation. By comparing with the experimental results obtained using the Tandem DMA technique described in Hummes et al. 1996, it was reported that the Nano-DMA was performing well in the designed size range and its transfer function agreed well with the numerical prediction.

Seol *et al.* (2002) designed and constructed an adjustable-column length differential mobility analyzer (ACLDMA) for wide particle size range measurements. It was capable of measuring particle sizes from 1 nm to hundreds of nanometers. Figure 1.21 shows a schematic diagram of the ACLDMA. The basic structure of the ACLDMA was similar to the DMA described by Knutson and Whitby (1975).

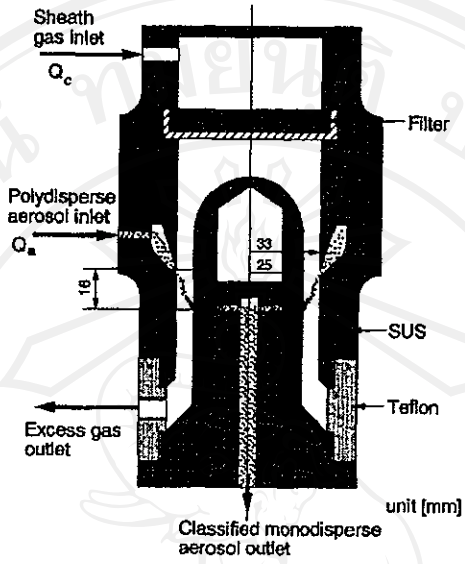

Figure 1.18 Schematic diagram of the LPDMA developed by Seto *et al.* (Seto *et al.* 1997).

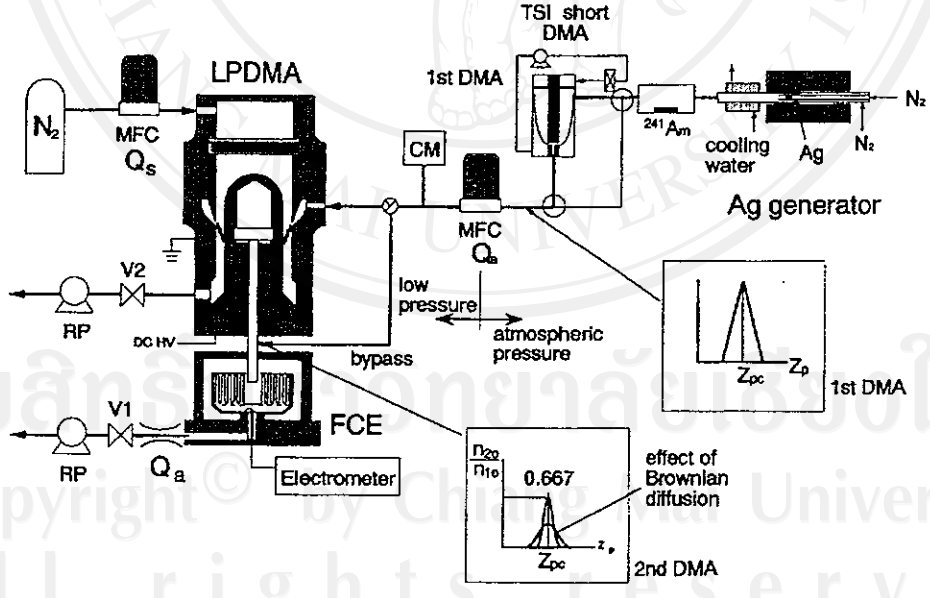

Figure 1.19 Experimental system for calibration of LPDMA (Seto *et al.* 1997).

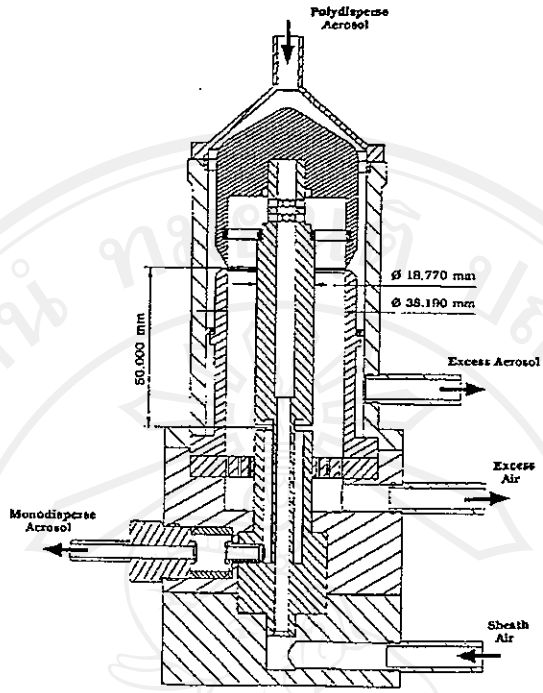

Figure 1.20 Schematic diagram of the Nano-DMA developed by Chen *et al.* (Chen *et al.* 1998).

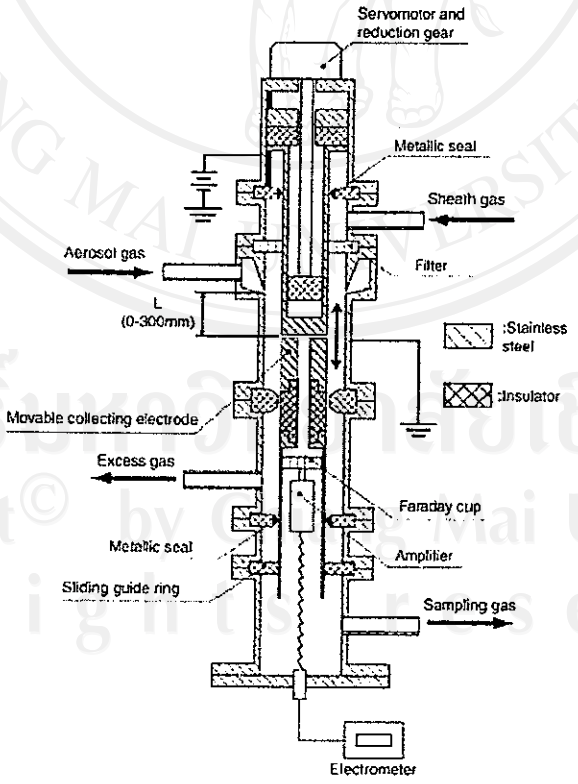

Figure 1.21 Schematic of an adjustable-column length DMA (ACLDMA) (Seol *et al.* 2002).

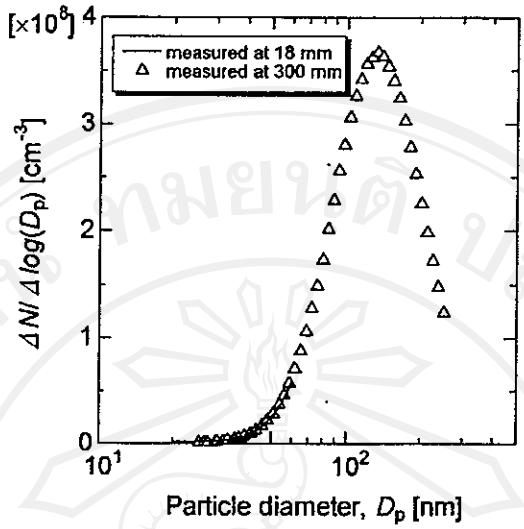

Figure 1.22 Particle size distribution measured with the ACLDMA when L = 18 and 300 mm (Seol *et al.* 2002).

The ACLDMA was characterized by an adjustable inner electrode whose length can be varied from 0 to 300 mm. The inner and outer electrode radii were 25 and 38 mm, respectively. The inner electrode was moved with a servomotor and reduction gear with a position accuracy of 0.3 μm. The position of the inner electrode was monitored with a laser displacement sensor with a resolution of 2 μm. From these characteristics and for L = 16 mm, the uncertainty of the mobility was ±0.0125 % of the set mobility. To minimize the eccentricity of the inner electrode, a pair of sliding guide rings was used. Metallic seals were used to separate the classification and drive parts of the electrode. The ACLDMA also used a built-in Faraday cup electrometer to measure the total particle current. The Faraday cup was placed inside the inner electrode of the DMA. The classification characteristics of the ACLDMA were investigated by two methods: a tandem DMA method and the C_{60} monomer measurement method. The tandem DMA method was used to evaluate the controllability of the column length. NaCl particles were prepared by using NaCl evaporation and recondensation to form particles, which were classified in a reference DMA to produce 10 nm particles. These particles were fed into the ACLDMA, and the mobility distribution was measured at column lengths from 0 to 300 mm. The reference DMA and ACLDMA were both operated with sheath air flow of 10 lpm and aerosol flow of 1 lpm. The C_{60} monomer measurement method, which was an inherently monodispersed spherical nanoparticle, was used to produce standard nanoparticles less than 3 nm in diameter. For this test, C_{60} powder (purity: 99.98%) contained in a quartz crucible was vaporized under a N_2 atmosphere in a quartz tube heated by an electrical furnace. The C_{60} monomer thus produced was passed into the ^{241}Am neutralizer using N_2 gas at a flow rate of 2.8 lpm for charging. It was reported that the resolution of the DMA obtained for a C_{60} monomer (1 nm in diameter) agreed with that expected by the diffusing transfer theory (Stolzenburg 1988) when $L \leq 150$ mm. The height of the transfer function showed anomalous dependence on L, i.e. the height reaches a maximum at L = 36 mm, which cannot be explained by diffusing transfer theory and/or space charge effect. Figure 1.22 represents particle size distribution of NaCl particles that were formed by evaporation of NaCl powder at 700^0 C were measured with the ACLDMA when L = 18 and 300 mm. The particle size obtained at L = 18 mm ended at approximately 30 nm, while the size distribution obtained at L = 300 mm extended up to approximately 270 nm.

1.2.3 Development of Electrical Mobility Analysis Based Instruments

In this Section, a description of already existing electrical mobility measuring instruments is given. There are several techniques and instruments that have been developed and are commercially available for measuring particle size. Each is built for different applications and for measuring different particle size ranges and different in operation. Only seven instruments will be presented due to their similarities to the electrical mobility spectrometer (EMS). Namely, these instruments are the Scanning Mobility Particle Sizer (SMPS) which consists of the Differential Mobility Analyzer (DMA) and the Condensation Particle Counter (CPC), the Electrical Aerosol Analyzer (EAA), the Electrical Aerosol Spectrometer (EAS) developed in Tartu University, the Electrical Low Pressure Impactor (ELPI), Engine Exhaust Particle Sizer (EEPS), Bipolar Charge Aerosol Classifier (BCAC), Fast Aerosol Spectrometer (FAS) and Differential Mobility Spectrometer (DMS).

(a) Scanning Mobility Particle Sizer

The Scanning Mobility Particle Sizer (SMPS), which is commercially available from TSI, based on the principle of electrical mobility classification (Whitby and Clake 1966; Knutson and Whitby 1975; Wang and Flagan 1990; Rosell-Llompart *et al.* 1996) and used to measure number-weighted particle size distributions in the range of 3 – 1000 nm. A schematic diagram of the SMPS is shown in Figure 1.23. The SMPS consists of three main parts: the particle charger, the differential mobility analyzer (DMA) and the detection system. As shown on the diagram, the SMPS uses a bipolar charger (neutralizer) before the DMA in order to bring particle charge levels to a Boltzmann equilibrium charge distribution. The polydisperse aerosols are then passed through the DMA near the inner surface of the outer electrode, which consists of a high voltage inner electrode concentrically surrounded by a grounded outer electrode. A laminar flow of particle-free sheath air (usually at a 10:1 ratio with respect to the aerosol flow rate) is passed through the DMA, near the inner electrode. Depending on their charge (positive and negative), particles are attracted or repelled by the inner electrode at different rates, depending on the electrical mobility of each particle. Particles of high electrical mobility precipitate close to the aerosol inlet while particles of lower mobilities precipitate further down the column. Particles within a narrow range of electrical mobility diameter, exit the DMA through the monodisperse sample flow (a circumferential slit on the inner electrode located downstream the aerosol inlet), these particles are referred to as the monodisperse aerosol. The monodisperse aerosols are then transferred to the condensation particle counter (CPC, see below) where the number concentration of the particles is measured. All the remaining particles exit the DMA via the excess flow. The time response of the SMPS is typically 60 – 120 seconds. The particle number concentration that the SMPS can measure range with particle size is approximately $10^4 - 10^9$ particles/cm^3.

(b) Condensation Particle Counter

The Condensation Particle Counter (CPC) is the widely used instrument for measuring total particle number concentration, regardless of particle size (Agrawal and Sem 1980). The CPC is an optical instrument. However, because the optical systems are not able of detecting particles with diameter less than 1 nm, particle growth is required. A schematic diagram of a CPC is shown in Figure 1.24. It consists of a horizontal saturator, a vertical condenser, focusing optics and collecting optics. As the particles enter the CPC, they are exposed to a heated alcohol reservoir and the whole mixture becomes saturated. The aerosol then passed through a condenser tube where the temperature is maintained well bellow the dew point of the alcohol-saturated mixture, forcing the alcohol into a state of supersaturation.

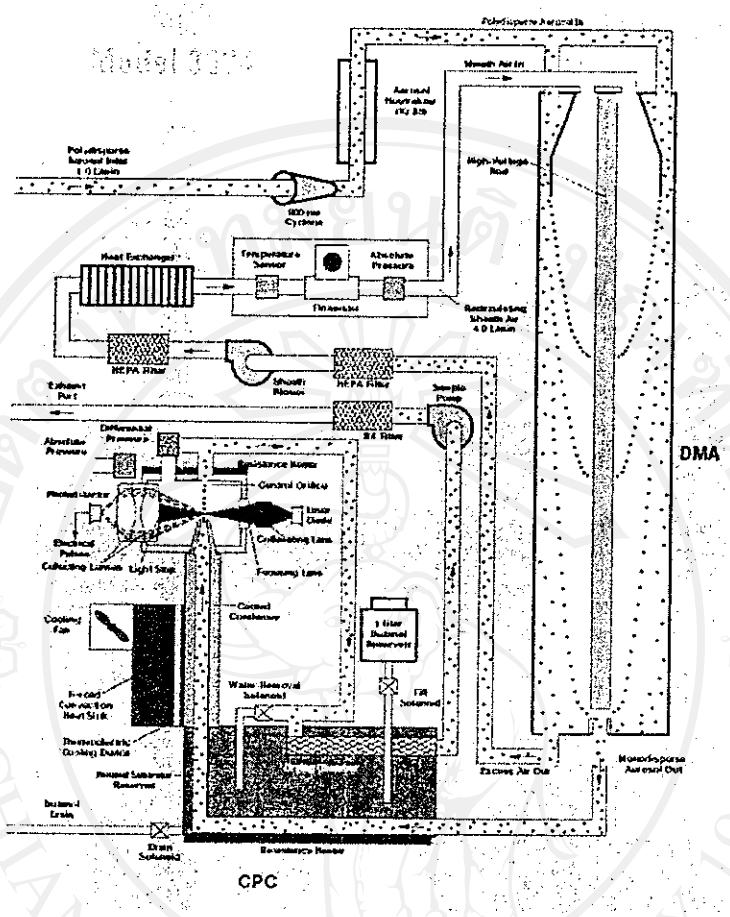

Figure 1.23 Schematic diagram of the Scanning Mobility Particle Sizer (TSI 2006).

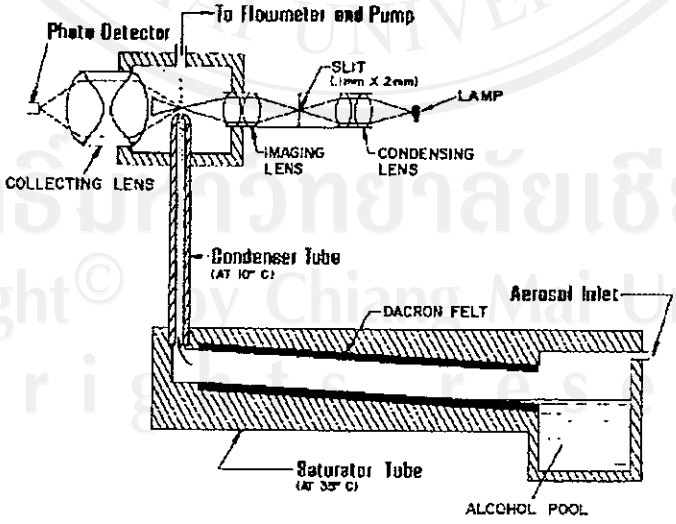

Figure 1.24 Schematic diagram of the Condensation Particle Counter (Agrawal and Sem 1980).

The supersaturated alcohol then begins to condense on the particles, causing them to grow in size from their various initial diameters to a relatively uniform final diameter of approximately 12 μm. Finally, the now larger particles are passed through the optical counter where their concentration is measured. TSI Incorporated produces many CPC models, the most popular of which are the model 3025A, capable of detecting particles as small as 3 nm at particle number concentrations up to 10^5 particles/cm^3 with the time response of 1 second, and the model 3022A, which is capable of measuring particles as small as 7 nm at particle number concentration up to 10^7 particles/cm^3 with the time response of 12 seconds.

(c) Electrical Aerosol Analyzer

The ancestor of the SMPS is the Electrical Aerosol Analyzer (EAA) manufactured by TSI. Originally described and tested by Whitby and Clark (1966), it was known as the Whitby Aerosol Analyzer (WAA) for the first year. The performance of EAA is based on the same principles with the SMPS. However, there are two main differences between these two instruments. The first is that particle charging is accomplished with corona-wire discharge, hence they acquire a unipolar charge (unipolar diffusion charging as discussed earlier). The second main difference is that instead of a particle counter that uses optical detectors, an electrical sensor is employed for particle measurement. The measurement is performed by first exposing the aerosol to unipolar gaseous ions in the diffusion charger and then charged particles are passed through the mobility analyzer are directed through as small slit at the outlet of the instrument to a Faraday-cage electrometer where the total charge of the aerosol is measured. The current measurements are then converted to particle number concentrations given the mean charge on the particles. Varying the collecting rod voltage in the mobility analyzer, particles of different mobility are detected by the electrometer, and the size distribution of the aerosol is measured. A schematic diagram of the EAA is shown in Figure 1.25. The instrument, originally designed and tested by Liu *et al.* (1974), was commercially available by TSI with some modification as described later by Liu and Pui (1975). Similar to the SMPS, the limitation of the EAA is the great amount of time required to estimate the aerosol size distribution. The TSI EAA requires 2 -3 minutes to measure the entire size distribution in 11 scanning steps.

(d) Electrical Aerosol Spectrometer of Tartu University

The Electrical Aerosol Spectrometer (EAS) developed at Tartu University is an instrument for measuring number-weighted particle size distributions in the range of 10 nm to 10 μm by electrical mobility methods (Mirme 1994; Tammet *et al.* 2002). The design of the EAS is shown in Figure 1.26. The EAS was designed on the full parallel measuring principle. The EAS contains two mobility analyzers, one provided with a weak electric field or diffusion charger (D-analyzer), and the other with a strong electric field charger (E-analyzer). High sensitivity has been achieved by unipolar charging of particles. The positive polarity of charge is used. The particles up to the diameter of 0.5 μm are resolved using ion diffusion charging. The particles of the diameter of above 0.3 μm are resolved using unipolar charging in a strong electric field. The mobility analyzers are the cylindrical capacitors consisting of particle repulsive inner electrode and particle collecting outer electrode. The collecting electrodes of the mobility analyzers are divided into isolated sections each of which is provided with an electrometric amplifier (electrometer). Each section together with its electrometer corresponds to a measuring channel of the spectrometer. The EAS has 32 measuring channels. Aerosol is sucked into the analyzers through the preconditioning facilities (laminarizers, dischargers) and through the charging zones of the chargers close to the inner (repulsive) electrodes. The charging conditions in the chargers are stabilised by feedback circuits.

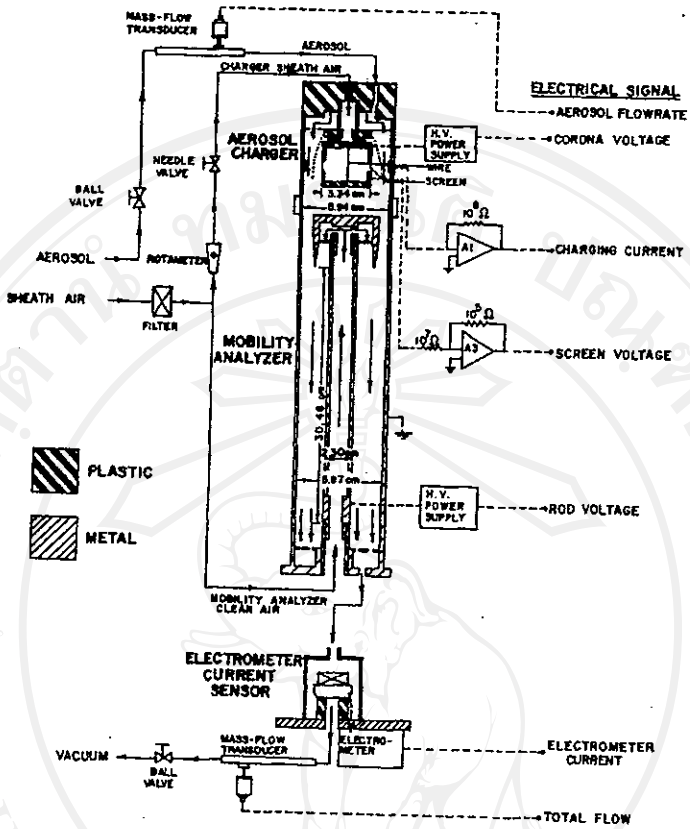

Figure 1.25 Schematic diagram of the Electrical Aerosol Analyzer (Liu and Pui 1975).

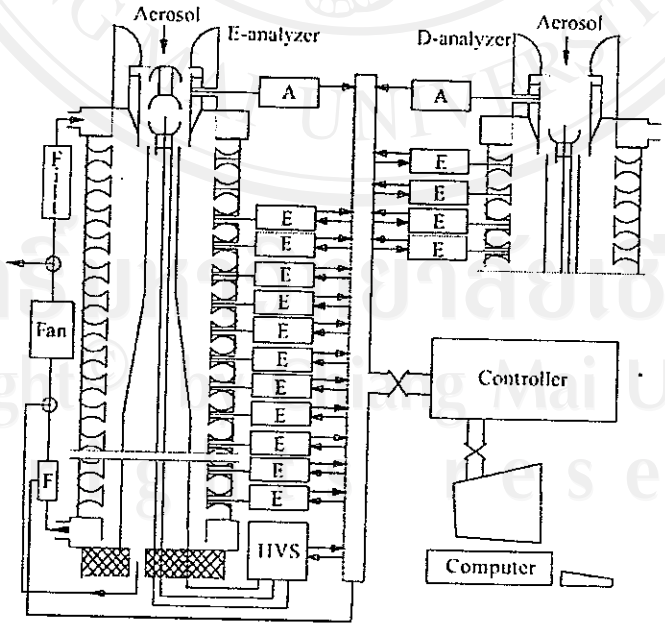

Figure 1.26 Schematic diagram of the Electrical Aerosol Spectrometer of Tartu University (Tammet *et al.* 2002).

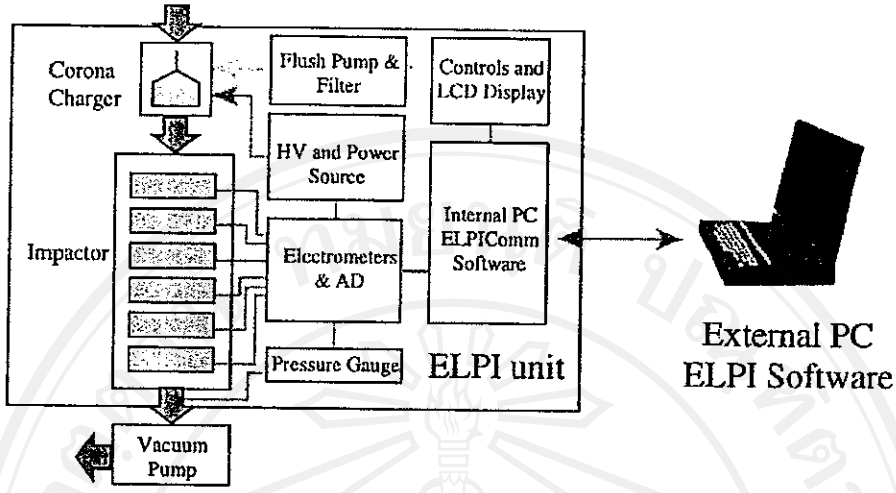

Figure 1.27 Schematic diagram of the Electrical Low Pressure Impactor (Marjamaki *et al.* 2000).

The charged particles moving in the radial electric field of the mobility analyzers precipitate on the different sections of the mobility analyzers according to their electrical mobility. The electric currents carried over these sections by particles are measured by electrometers and form the output signals vector of the apparatus (apparatus record). The time uncertainty of measurement is reduced by measuring the same aerosol sample, synchronously with its movement on in the analyzer. A special controller has been designed to control the measurement and record data. The maximum resolution of the electrometric signal is 0.25 mV making about 2.5×10^{-16} A on the scale of the aerosol electric current. The main spectrometer parameters such as charging currents and air flow rates are also controlled. The time response of the EAS is approximately 1 second for the fastest sampling rate. However, for statistically significant size distribution measurement a typical time of 5 seconds is required. The particle number concentration that the EAS can measure ranges with particle size; this is 10^2 - 10^5 particles/cm^3 for particles as small as 10 nm and 2×10^{-2} - 5×10^1 particles/cm^3 for particle up to 10 μm.

(e) Electrical Low Pressure Impactor

The Electrical Low Pressure Impactor (ELPI), which is commercially available from Dekati, Finland, is a more recent instrument for measuring aerosol size distributions (Keskinen 1992; Keskinen *et al.* 1992; Marjamaki *et al.* 2000). The ELPI classifies particles based on their aerodynamic diameter. It combines the principles of electrical detection with size classification by impaction. The ELPI can determine aerosol spectra in the size range of 0.030 - 10 μm. Figure 1.27 shows a schematic diagram of the ELPI. The sample aerosols first pass through a unipolar corona charger. The charged particles then pass into a 12 low pressure cascade impactor with electrically isolated collection stages. The electrical current carried by the collected charged particles into each stage is measured by a multichannel electrometer is related to number concentration. Combining the current reading from every impaction stage, the size distribution of the aerosol sample is obtained. The measurement system is controlled and the data sampled by a personal computer. An advantage of the ELPI is that particles in the different stages of the impactor can be collected on substrates for microscopic analysis or additional measurements of their mass and composition. The ELPI was originally developed as a device for monitoring of flue gas in industrial and power generation smoke stacks.

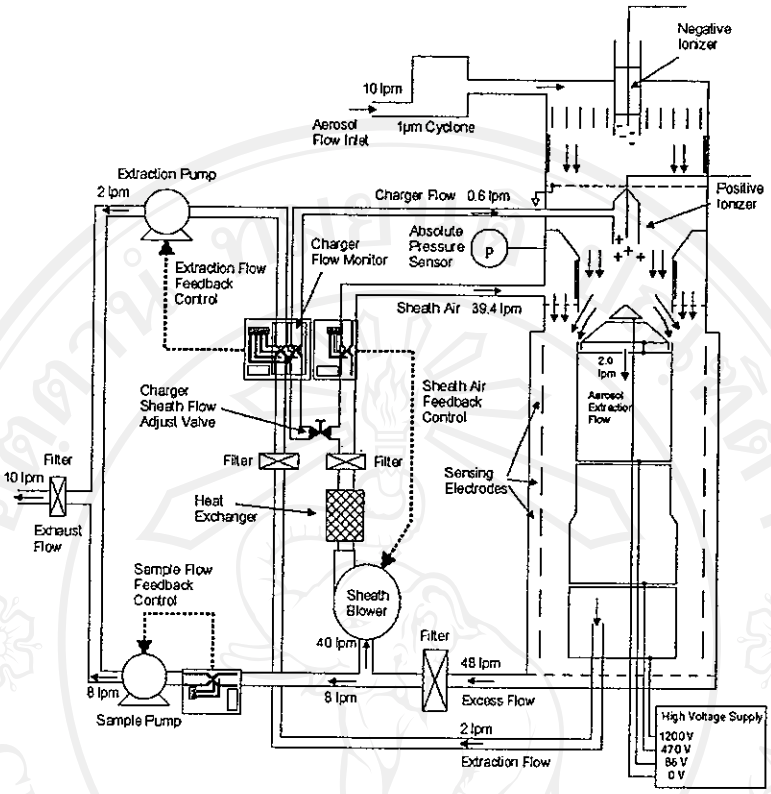

Figure 1.28 Schematic diagram of the Engine Exhaust Particle Sizer (TSI 2006).

The time response of the instrument is of the order of 2 seconds. The ELPI can measure particle size with number concentration in the range from approximately 10^2 – 10^7 particles/cm^3.

(f) Engine Exhaust Particle Sizer

The Engine Exhaust Particle Sizer (EEPS) is a very recently announced instrument for fast response aerosol measurements in the range of 5.6 to 560 nm in diameter. The EEPS, which is commercially available from TSI, is similar to the EAS described above. The schematic diagram of the EEPS is shown in Figure 1.28, employing a unipolar diffusion charger to charge the incoming aerosol sample and an "inside-out" electrostatic classifier to separate particle according to their electrical mobility, it detects and measures particle concentration by a series of 22 electrometer rings along the column classifier. Particle size distributions are then estimated using the current measurements from the individual channels and a data inversion algorithm. The time response of the EEPS is approximately 100 milliseconds.

(g) Bipolar Charge Aerosol Classifier

The Bipolar Charge Aerosol Classifier (BCAC) developed at Brunel University, UK is an instrument for measuring aerosol bipolar charge distributions by electrical mobility technique (Kulon *et al.* 2001). A schematic diagram of the BCAC is shown in Figure 1.29. The BCAC system incorporates a front-end cylindrical arrangement consisting of ten well-insulated sections.

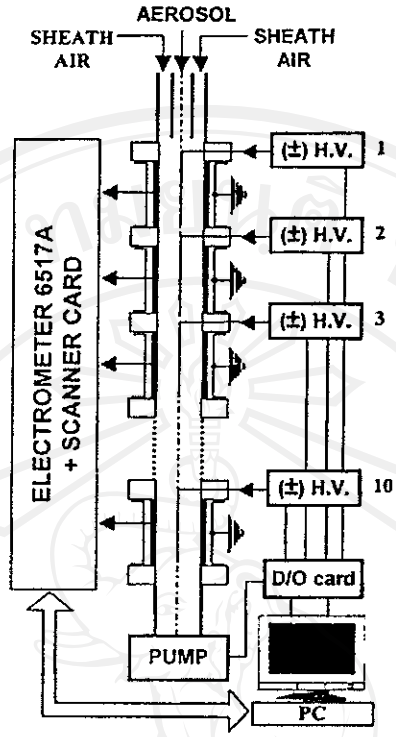

Figure 1.29 Schematic diagram of the Bipolar Charge Aerosol Classifier (Kulon *et al.* 2001).

Each of these sections is composed of a cylindrical capacitor with a coaxial wire electrode maintained at a DC high potential. Aerosol is drawn through the separator using a suction pump, and subject to an appropriate electric field. Depending on the electric field distribution and air flow rate, charged particles of the same polarity as that of the potential applied to the wire electrodes are deflected toward an outer collecting wall and give up their charge. The accumulated charge on each of the electrodes are measured with a Keithley 6517A electrometer incorporating low current, 10 channel 6522 scanner card. All devices are interfaced to a personal computer via an IEEE-488 interface and PIO card and controlled by TestPoint software. The time response of the BCAC is approximately 10 sec.

(h) Fast Aerosol Spectrometer

The Fast Aerosol Spectrometer (FAS) developed at University of Cambridge is an instrument for the fast measurement of number-weighted aerosol size distribution for particles in the size range from approximately 1 – 100 nm by electrical mobility method (Graskow 2001). A schematic diagram of the FAS is shown in Figure 1.30. The overall design and operating principle of the FAS is similar to the EAS described above. However, there is difference between the two instruments: particle charging of the FAS is accomplished by photoelectric charger resulting in bipolarly charged aerosol particles. The FAS is composed of the aerosol charger, the size classification column and the signal current detector. Particle charging was carried out by exposing the aerosol sample to intense monochromatic UV light which results in photoelectric ejection of electrons from particle surfaces. The UV lamp used is a KrCl excimer which produces photons at a wavelength of 222 nm (hv = 5.6 eV) (Graskow 2001). It is powered by an AC source of a ±4 kV triangle wave pulse at a frequency of 40 kHz with charging residence time is approximately 100 ms.

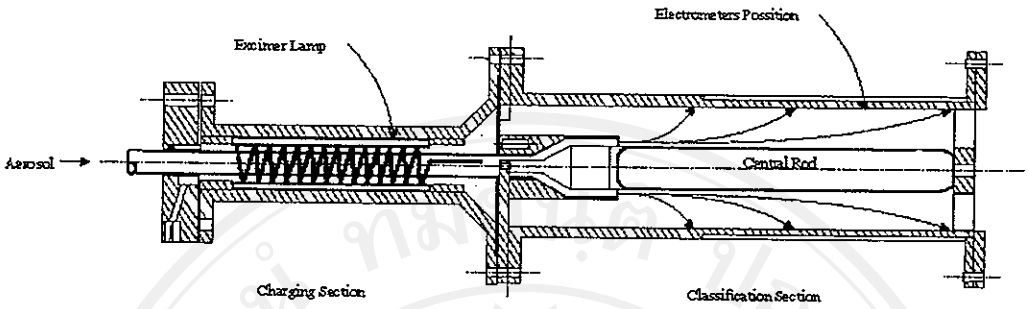

Figure 1.30 Schematic diagram of the Fast Aerosol Spectrometer (Graskow 2001).

After the charger, the charged particles then enter the size classification section is based on the same principles used by DMA. The FAS classifier consists of two coaxial electrodes with the central rod is maintained at a positive high voltage range varies between 1 and 10 kV and the outer chassis of the classification section being grounded. The central rod is made of a stainless steel rod with 20 mm diameter and outer chassis is made of a stainless steel tube with 50 mm diameter and 150 mm in length. There are two streams which are the aerosol and sheath air flows, the charged particles are introduced into the classification section near the central rod by a continuous flow of air, and surrounded by a sheath air flow. Since the central rod is kept at a positive voltage, the charged particles are deflected outward radially according to their electrical mobility and they are collected on a series of eleven isolated electrode rings at the inner surface of the outer chassis of the FAS classifier. Each electrode ring was 10 mm wide with a 0.6 mm gap in between the electrometer rings for isolation. The electric currents due to the charged particles are measured by an electrometer and are then translated to particle number concentrations corresponding to the size range collected on each electrode ring. The electrometer circuit used for current measurement in the FAS employs the amplifier Analog Device AD549L. A schematic diagram of the FAS electrometer is shown in Figure 1.31. This circuit gives an output of 10 mV/pA of input current signal. It was reported that the time response of the FAS is approximately 38 milliseconds.

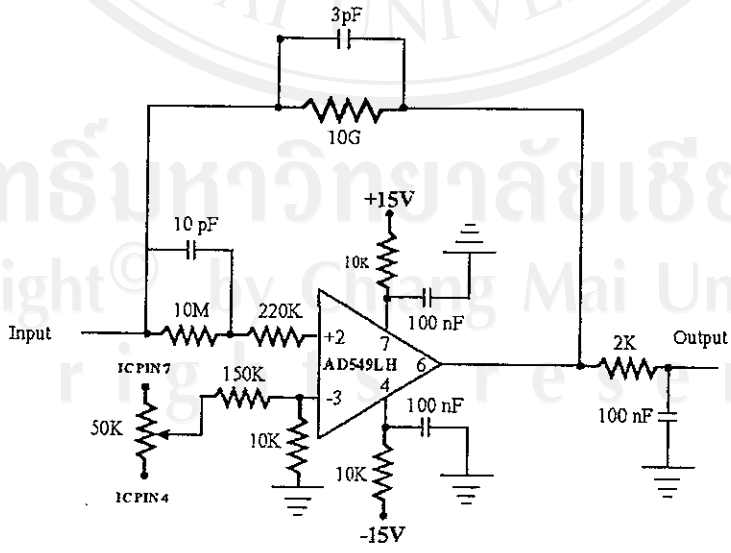

Figure 1.31 Schematic diagram of the electrometer circuit of the FAS (Graskow 2001).

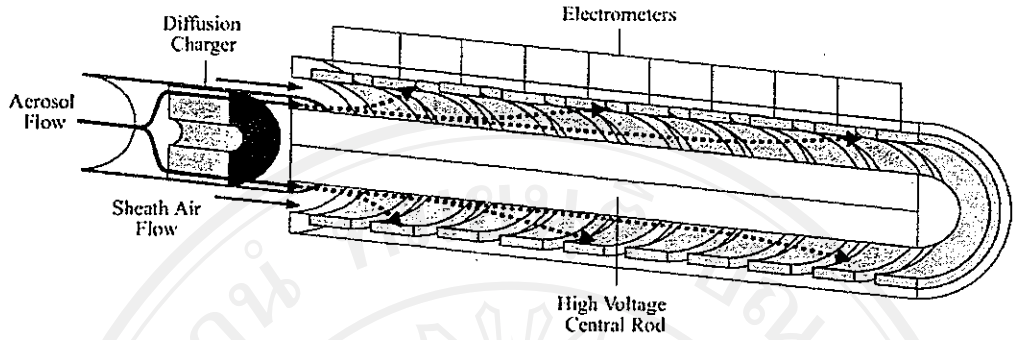

Figure 1.32 Schematic diagram of the Differential Mobility Spectrometer (Biskos 2004).

(i) Differential Mobility Spectrometer

Differential Mobility Spectrometer (DMS) manufactured by CAMBUSTION, UK, is similar to the FAS described above (Reavell *et al.* 2001; Biskos 2004). However, there are two main differences between the two instruments: first, particle charging is accomplished by a corona-wire diffusion charger resulting in unipolarly charged aerosol particles, and second, the DMS operates at pressure below ambient (0.25 atm). The DMS is something of a hybrid of the DMA and the ELPI. Figure 1.32 represents a schematic diagram of the DMS: like the ELPI, particles in a sample are charged by a corona charger, like the DMA, they are classified by their electrical mobility. Like the ELPI, the quantity of classified particles in each size range is deduced from the charge flow to a set of electrometers (Reavell *et al.* 2001). The DMS is capable of fast response aerosol measurements in the range of 5 to 1000 nm in diameter, with a time response of 200 milliseconds. The DMS consists of three main parts; the particle charger, the classification column, and the detection system. Aerosol particles are passed through a corona-wire diffusion charger, a Hewitt-type single-wire corona charger, to charge the sample aerosol prior entrance to the column. The charger is maintained at 0.25 atm in order to increase mobility resolution for particles with diameter greater than 100 nm (Reavell *et al.* 2001). Following the charger, the charged particles enter the classification column. The classification column is 700 mm long with an internal diameter of 53 mm. The DMS column (operating at the same pressure as the charger) consists of two concentric electrodes with an axially increasing electric field established in between. This varying electric field is created by a linearly increasing (from the aerosol inlet to the end of the column) potential along the central rod. This varying electric field results into a better resolution of particle size distribution. The actual number concentration of the charged particles is determined by a series of 26 metallic rings connected to sensitive electrometers placed in the inner surface of the outer electrode of the column. The first eight rings from inlet are 14.5 mm wide, while the rest have a width of 29.5 mm. The start of the first electrometer ring is located 18.5 mm downstream of the aerosol inlet, and a 0.5 mm gap is allowed between the electrometer rings for isolation. Figure 1.33 shows the circuit of the DMS electrometers with 2 fA sensitivity. The actual size distribution of the input aerosol can be determined by deconvoluting the electrometer current readings. The DMS can measure particle size with number concentration in the range from approximately $1 \times 10^3 - 4 \times 10^7$ particles/cm^3.

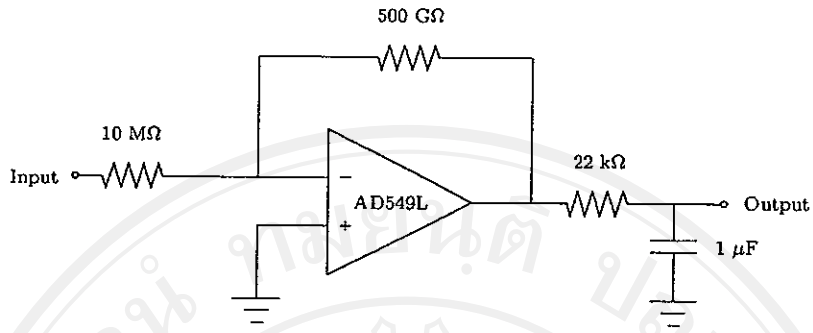

Figure 1.33 Schematic diagram of the electrometer circuit of the DMS (Biskos 2004).

1.3 Aims of the Study

- To investigate the aerosol transport under influence of an electric field and the factors which affect the aerosol measurement in sub-micrometer size range i.e. dimension of the instrument, fluid flow rate, electric field strength, particle charge distribution, and particle losses
- To design, construct, and test the prototype of an electrical aerosol size measurement system using electrical mobility technique
- To experimentally evaluate performance of the instrument and compare with the standard aerosol measuring instrument

1.4 Benefits of the Study

- Clear explanation of the factor which affect to the aerosol measurement in sub-micrometer range can be achieved
- Clear explanation the aerosol transport under influence of an electric field can be achieved
- Components and control system and data acquisition and processing system of the instrument can be obtained
- The prototype of an aerosol size measurement system using electrical mobility technique can be obtained

1.5 Scope of the Study

- An electrical mobility technique is used in this study
- Study of the experimental factors were as follows;
  - Central rod voltage in the range of 1.0 to 3.0 kV
  - Aerosol flow rate in the range of 1.0 to 3.0 l/min
  - Sheath air flow rate in the range of 5.0 to 10.0 l/min
- This instrument design for the laboratory test
- Components of the instrument system consist of a size selective inlet, a particle charger, a size classifier, a signal current detector and a computer controlled data acquisition and processing system will be constructed
- In this study, the particle shape is spherical and uniform distribution will be assumed
- The particle size in the range of 10 to 1000 nm will be considered
- Software for the instrument control and data acquisition and processing system will be developed

1.6 Thesis Outlines

The text of this thesis is divided into six Chapters and four Appendices. The first Chapter (current chapter) serves as an introduction to the thesis addressing the statement and significance of the problem, the literature review of the existing electrical aerosol instruments, and the objectives of the study. Chapter 2 gives some of the basic fundamentals of aerosol particle properties and theories needed to characterize the performance of the electrical mobility spectrometer (EMS). These include the aerosol properties, the particle motion in gases, the particle charging mechanisms, and the flow field and electric field modeling. A detailed description of the EMS and the analytical and numerical modeling methods used to predict the performance of individual components of the EMS are provided in Chapter 3. These are the size selective inlet, the particle charger, the mobility classifier, the electrometer, and the data acquisition and processing system. A brief description of the primary apparatus and procedures used throughout the experimental work of the present study is presented in Chapter 4. A discussion on the experimental results against theoretical predictions of the EMS performance are presented and described in Chapter 5. Finally, Chapter 6 presents the main conclusions of the present work and provides recommendations for further works.

Appendix A gives the detailed drawing for the EMS including the size selective inlet, the corona-needle charger, the corona-wire charger, and the mobility classifier. Appendix B provides the schematic diagram of the computer interface and electrometer circuits. These include the I^2C computer interface circuit schematic, the DC power supply circuit schematic, the electrometer circuit schematic, and the relay switching circuit schematic. The operation manual of the EMS is provided in Appendix C. Finally, a list of publications included in the thesis is also presented in Appendix D.